

Experimental evaluation of residual tensile strength of hybrid composite aerospace materials after low velocity impact

 The corrections made in this section will be reviewed and approved by journal production editor.

Mahdi **Damghani**^{a,*} mahdi.damghani@uwe.ac.uk, Nuri **Ersoy**^a, Michal **Piorkowski**^a, Adrian **Murphy**^b

^aDepartment of Engineering Design and Mathematics, University of the West of England (UWE), Bristol, BS16 1QY, UK

^bSchool of Mechanical and Aerospace Engineering, Queen's University Belfast (QUB), Belfast, BT9 5AG, UK

*Corresponding author.

Abstract

Although much work has considered hybridised Carbon and Glass Fibre Reinforced Polymers to positively influence the performance of composite structures when subjected to transverse impact loading, there is limited understanding considering low energy impact levels ($\leq 10\text{J}$) - in particular how variation in impact energy influences damage formation and post impact tensile strength. Herein, low velocity impact and residual tensile strength after impact tests are completed on four laminate designs (one pure Carbon laminate layup and three hybrid Carbon and Glass layups). Three repeat tests and three graduated low energy level impacts ($\leq 10\text{J}$) are considered along with pristine laminate performance. The impact response was evaluated in terms of surface damage size by visual inspection, and the evolution of peak force and stiffness with impact energy level. The contribution of this paper is the first presentation of a detailed experimental study on the tensile performance of hybrid composite materials subjected to a graduated range of low energy level impacts. The methodical experimental work demonstrates how the hybrid layup influences the scale and form of damage. By distributing the glass plies through the laminate, as opposed to clustering the glass plies at the inner or outer mould surfaces, more favourable residual tensile strength and strain to failure is demonstrated.

Keywords: Carbon fibre reinforced polymers; Glass fibre reinforced polymers; Hybrid composite laminates; Low velocity impact; Barely visible impact damage; Residual tensile strength

1 Introduction

The laminated construction of fibre reinforced composites and the characteristics of their constituent properties (fibre and matrix) often makes their structural performance sensitive to transverse impact loading. Moreover, impact laminate damage is not always visible on the surface of the material. As a result, conservative design philosophies are employed which assume damage and adjust down the pristine material properties for design. Thus, it is typically not possible to translate the full benefits of the material properties into product weight savings or strength improvements. As a result, much research has been carried out to understand the phenomenon and improve the impact resistance and damage tolerance of fibre reinforced composite laminates. One stream of this research is hybridised laminates, typically combining laminae of different fibre (e.g. Carbon and Glass) within a single matrix polymer. Laminate hybridisation research has demonstrated the potential to reduce the damage resulting from impact and increase the structural performance of damaged laminates.

Significant research has examined the benefits of hybridising stiff plies with more compliant plies with greater strain to failure. Much of the available research has considered impact and post-impact compression strength, with significantly less work on post-impact tensile strength. Although very few structures during their service are subjected to a single direction of structural loading, laminates generally have lower structural performance subjected to compression loading. Hence, the bias in the volume of literature towards compression scenarios. Moreover, individual studies rarely consider evenly graduated impact energy levels and thus the understanding of the influence of impact energy on the formation of hybridised laminate damage and post impact tensile strength is very limited.

Thus, the aim of this paper is to investigate how impact damage and post impact tension strength behaviour vary with impact energy, and quantify the influence of laminate stacking sequence on this behaviour. Herein, an extensive experimental study is undertaken to investigate and compare the behaviour of three configurations of hybrid woven Carbon and Glass composite laminates.

2 Background

This section introduces the current state of the art in aerospace design with composites, impact damage and approaches to mitigate the associated effects on structural performance.

2.1 Fibre reinforced composite laminates in aircraft design

Fibre reinforced composite laminates are now critical in both heavily and lightly loaded aerospace structures, e.g. wing structures, control surfaces. Impact events on such structures can result in two classifications of damage, i.e. Barely Visible Impact Damage (BVID) and Visible Impact Damage (VID). BVID is subjective by nature and is often caused as a result of low velocity impact (4–8 m/s) and energy of up to 50 J. This type of damage is small at the laminate surface but with the potential to be larger below the surface with damage including subsurface delaminations with multiple transverse shear cracks. Such BVID may not be found

during heavy maintenance by general visual inspection [1,2]. Hence, BVID in unrepaired structure should not reduce the strength below the ultimate design strength, and should not result in detrimental damage growth during the aircraft's Design Service Goal (DSG), i.e. the period of time (in flight cycles/hours) during which the structure will be reasonably free from significant fatigue damage.

VID, on the other hand, is associated with higher impact energy levels leading to significant visible fibre breakage in addition to delaminations and transverse shear cracking. The magnitude of delamination also increases through the thickness. VID in unrepaired structures must withstand the aircraft design limit loads without failure, and with no detrimental damage growth during fatigue cycling representative of the structure's inspection interval. Furthermore, the damaged airframe must be able to support residual strength loads until the damage is found and repaired. Similar to BVID, this type of damage needs to be validated by repeatable testing [2,3].

At present, the integrity of composite aerostructures is determined against strain/stress allowables [4]. In practice, pristine strain/stress allowables are knocked down by semi-empirical factors which allow the creation of damage tolerant designs by accounting for such properties as Compression After Impact (CAI), Tension After Impact (TAI) and Shear After Impact (SAI). The knock down factors are often within the range of 40%–60% of pristine values leading to the design of much thicker laminates and heavier structures. To minimise the weight penalty resulting from impact damage, the current industrial practice makes use of hybrid CFRP-GFRP laminates in aircraft wing construction, e.g. AIRBUS A350-XWB. From this perspective, 1 to 2 GFRP plies are placed on the outer mould surface of a purely CFRP laminate wing skin; where these plies act as a protective layer for the CFRP laminates against accidental impact. However, as the primary purpose of these additional plies is to reduce damage from impact, the load bearing capacity of the GFRP plies are typically ignored, thus adding extra weight to the structure. Thus, there is a clear need to better understand the impact resistance of hybridised laminates as well as their potential influence on strength once the laminate is damaged.

2.2 Laminate impact and post-impact tensile behaviour

In general researchers have found many parameters which influence contact behaviour and damage size in laminated composites. For example, impactor shape [5] and the laminate boundary conditions [6] are known to influence impact response and damage. Moreover, the thickness of the laminate and the material type (fibre and matrix) plays a crucial role in the contact behaviour and damage size. The influence of layup patterns on the impact behaviour of composite laminates has also been widely studied, but with less consensus. Some researchers believe that layup pattern does not play an important role on impact damage behaviour [7], whereas many others [8,9] argue that layup has a significant influence.

Focusing on residual tensile strength, Cestino et al. [10] studied the residual tensile strength and shear/uniaxial buckling performance of composite laminates after low velocity impact (4.6J–27.4J). The study examined panels of quasi-isotropic layup and found reductions of the order of 10–20% for panels impacted at lower energy levels. At higher energy levels reductions of the order of 50–70% were found for the ultimate tensile load. Zhou et al. [8] also studied the residual tensile strength of CFRP specimens after impact. They concluded that residual strength was closely related to the impact energy, with the strength decreasing rapidly at the high

impact energy studied (25.1 J by 31.3%–45.5%). Since the residual tensile strength of the laminates mainly depends on the damage status of the fibres in the loading direction, they proposed to place the plies with the fibres in the loading direction near the centre of the laminates to reduce the effect of low-velocity impact on the strength.

2.3 Improving laminate impact and post-impact performance

The impact resistance and damage tolerance of fibre reinforced composites can be enhanced by improving fibre/matrix interfacial adhesion, matrix modification, and fibre hybridisation [11]. It is worth noting that the brittle nature of fibres and the commonly employed epoxy matrix is one of the important factors for susceptibility to delamination in modern fibre-reinforced composites. For example, Glass Fibre Reinforced Polymer (GFRP), despite having lower stiffness and strength than CFRP, has higher strain to failure performance. This more ductile tensile characteristic benefits laminate behaviour in terms of impact energy absorption and damage containment [12–16]. Thus, with respect to hybridisation with high strength, high stiffness fibres, such as Carbon fibre, Glass fibres are a particularly good option. In addition, hybridising with individual plies of Carbon and Glass offer benefits from the viewpoint of cost, availability and ease of processing. Research has therefore considered hybrid carbon/glass fibre composites [17–19], and demonstrated improved damage tolerance. Hence, even though a fibre hybridisation method is an indirect approach to improve damage tolerance (in contrast to directly enhancing the matrix properties) it has notable cost and implementation advantages.

Liu et al. [19] carried out a comparative performance assessment on hybrid UD/woven composite laminates and an equivalent UD-only composite laminate. The results showed that the use of woven plies on the surfaces of a laminate had a small, but measurable, positive influence on the residual strength in a CAI test. He et al. [20] investigated impact and residual flexural strength of hybrid sandwich structures with CFRP skins and aluminium corrugated cores. Both the residual flexural strength and stiffness decreased significantly when the impact energy was lower than 10 J, while there was a slight reduction with a further increase in the applied impact energy. Yahaya et al. [21] investigated the ballistic impact properties of a woven Kenaf–Kevlar hybrid composite. The damage properties of the tested samples were also analysed. They proposed that it was possible to obtain higher energy absorption through appropriate hybrid laminate design, employing cheaper woven Kenaf for partial substitution of Aramid fibres. With the increase in Kenaf content, the ballistic properties of the hybrid composites were decreased.

Despite the considerable amount of scientific research into hybrid composite laminates including significant research programmes, e.g. HiPerDuct [22–25], there is limited published data on the residual tensile strength of hybrid pre-impregnated woven CFRP-GFRP laminates after low velocity impact. The reason is partly associated to the notion that low velocity impact does not lead to fibre fracture and hence does not have a critical influence on the residual tensile strength. However, low velocity impact could lead to splits in the off-axis plies that run from the free edge and could join up via delamination to form a characteristic staircase pattern, providing a fracture path without necessarily involving fibre fracture [26,27].

Amongst such studies is the work of Reddy et al. [28]. In this work hybrid laminate configurations of carbon and E-glass fibres were subjected to high velocity projectile impact. They demonstrated 17% improvement in

energy absorption for glass/carbon laminates (ratio of 50:50) over pure carbon laminate designs. Zhang et al. [29] investigated different E-glass/woven carbon fibre hybrid laminates. They demonstrated improved post impact strength for glass/carbon laminates (ratio of 50:50). However, stacking sequence design did not demonstrate a noticeable influence on the tensile properties, but did significantly affect the flexural and compressive properties. Rhead et al. [30] investigated the influence of stacking sequence, both position and number of glass layers, on the damage resistance and CAI strength of glass/carbon laminates. Hybrid laminates were shown to display increases in structural efficiency of up to 51% for 12J and 41% for 18J impacts in comparison to CFRP laminates with identical impact energies. They concluded that the extent to which the hybrid laminates outperformed the CFRP laminates in the CAI tests was dependent on the stacking sequence and through-thickness positioning of the glass layers. Table 1 summarises some of the research on residual strength of hybrid composites after impact. To the authors best knowledge, no research has systematically varied impact energy and established how impact damage and structural behaviour under tensile loading changes for hybrid laminates. The reader may refer to Refs. [31,32] for a broader review of existing literature on hybrid composites.

alt-text: Table 1

Table 1

 The presentation of Tables and the formatting of text in the online proof do not match the final output, though the data is the same. To preview the actual presentation, view the Proof.

A summary of research on residual strength of hybrid composite after impact.

Researcher	Impact energy (Joules)	Specimen size (mm x mm)	Hybrid type	Residual strength studied	Main outcomes
Rhead et al. [30]	12, 18	125×75	CFRP-GFRP	CAI & buckling (Experimental)	On average hybrid laminates enhanced CAI by 148% (for 12J) & 133% (for 18J)
Naik et al. [16]	20	127×127	CFRP-GFRP	CAI (Experimental)	Higher CAI and lower notch sensitivity for hybrid laminates compared to CFRP laminates
Meng et al. [42]	High velocity	50×50	CFRP-GFRP	Residual velocity (Numerical)	Improved performance of hybrid laminate compared to purely carbon laminate
Ismail et al. [43]	5, 10, 15 & 20	300×300	Flax-Carbon & Flax-Glass	CAI (Experimental)	Flax-Glass enhance CAI by 135% compared to Flax-Carbon
Dhakal et al. [44]	5, 10 & 15	100×100	flax & basalt fibres with Polyfurfuryl Alchhol (PFA) bio-resin	Flexural test (Experimental)	Improvement of impact performance but no comparison with non-hybrid composites was made

Liu et al. [19]	10, 17 & 25	150 × 100	UD CFRP-Woven CFRP	CAI (Experimental & Numerical)	3.3% improvement for 25 J impact
Jefferson et al. [45]	2.17	150 × 100	GFRP-BFRP	CAI (Experimental)	Hybrid laminates underperformed compared to pure GFRP laminates
Naseer et al. [46]	100	pipe	CFRP-CFRP	CAI (Experimental)	Hybrid laminates outperformed pure CFRP laminates

2.4 Summary

In summary, fibre reinforced composite laminates must be designed considering impact. To date, commonly employed fibre and matrix materials can't achieve their full potential but fibre hybridisation offers some immediate advantages. However, there is limited experimental work and understanding on how impact damage and post impact tension strength behaviour varies with impact energy, and how this behaviour will be influenced by laminate stacking sequence.

3 Materials and methods

3.1 Composite material and fabrication

The materials used in this study were woven pre-impregnated carbon fibre (AX-5180), and a woven pre-impregnated glass fibre (AX-3180) with mechanical properties given in Table 2. It is worth noting that in the absence of manufacturer's data sheet, the mechanical properties are obtained by the authors. Both carbon and glass prepreps consist of 54% fibre by volume (60% by weight) and have compatible resin contents enabling simultaneous curing in the hot press. For each impact energy level, four configurations of laminates were manufactured and three specimens for each configuration were considered to capture repeatability.

alt-text: Table 2

Table 2

 The presentation of Tables and the formatting of text in the online proof do not match the final output, though the data is the same. To preview the actual presentation, view the Proof.

Mechanical properties of both woven CFRP (AX 5180) and GFRP (AX 3180) fabric plies.

Mechanical properties	Units	AX 5180 CFRP	AX 3180 GFRP
$E_{11} = E_{22}$	MPa	73213.33	31745.00
G_{12}	MPa	4452.47	5442.04
S_t^a	MPa	649.67	570.43
S_c	MPa	590.00	514.30

S_s	MPa	87.00	62.00
Strain to failure	Strain	0.009	0.018
ν_{12} (Poisson's ratio)	N/A	0.04	0.14
t_{ply}^b	mm	0.20	0.225

Table Footnotes

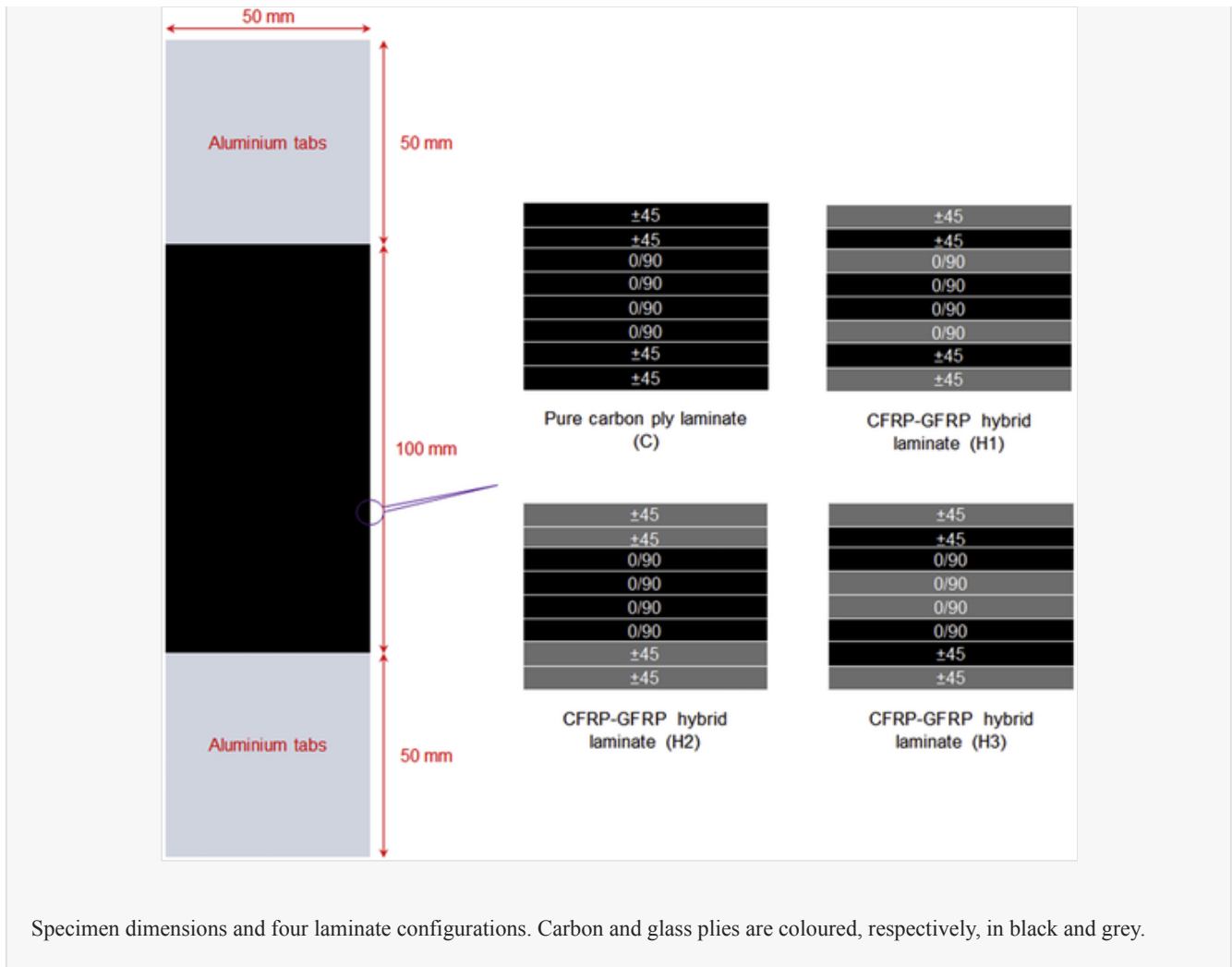
^a t, c and s subscripts denote strength of ply in tensions, compression and shear respectively.

^bCured ply thickness.

As depicted in Fig. 1, each configuration is symmetric and balanced in lay-up comprising 8 plies in total. Each laminate configuration was hand laid to form a plate and cured in a heated press for an hour at 120° Celsius under 1 bar pressure. The individual test specimens of 200×50 mm were then sectioned from the plate with a band saw cutter. The C configuration was comprised of purely woven carbon plies. The total thickness for the individual C specimens was measured as 1.6 mm. For the hybrid configurations, four of the carbon plies were replaced with glass plies having the same orientation. H1 and H3 configurations represented scattering GFRP through the thickness, Fig. 1. H2 laminates considered GFRP on the inner and outer mould surfaces typifying current industrial practice for wing skin design. The total thickness of the H laminates was measured as 1.7 mm.

alt-text: Fig. 1

Fig. 1



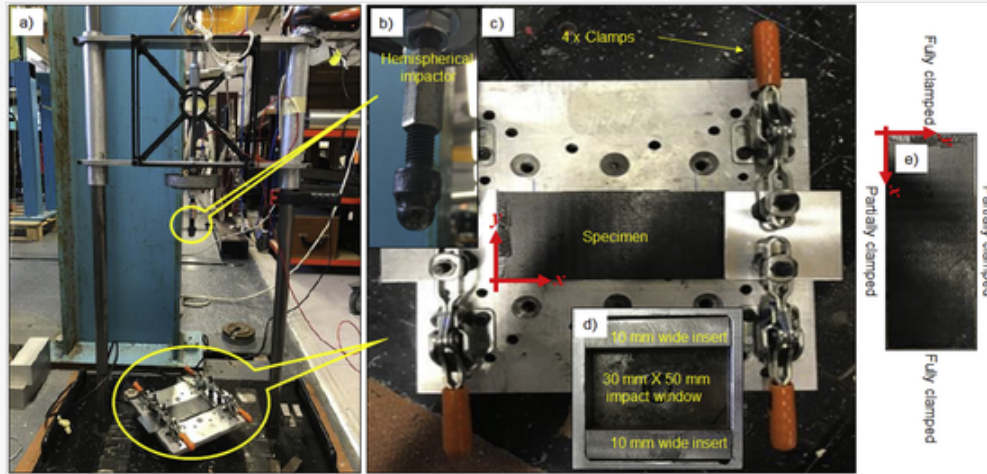
3.2 Impact fixture and impactor

The impact fixture included the cover plate and the supporting block as depicted in Fig. 2. The cover plate had an opening of 50 × 50 mm positioned at the centre of the specimen. The impact experiment set up was based on ASTM D7136 with variation to specimen geometry to reflect boundary conditions (BCs) similar to those found in aerospace structures such as wing panels where BCs are neither fully clamped nor simply supported. Hence, two 10 mm wide inserts were placed on both sides of the impact window under the laminates (see Fig. 2d). This led to BCs in which two edges could be assumed to be fully clamped and the other two (under inserts) to be in contact with the backing plate and neither fully clamped nor simply supported (see Fig. 2e). The base was secured by using a screw on mechanism to the bottom of the impact apparatus. The striker tip of the impactor was blunt and hemispherical in shape, with a contacting head diameter of 12.1 ± 0.05 mm. The impactor head and the guide mechanism had a combined mass of 1.82 kg. An additional, fixed mass of 1.00 kg was added to the impactor to give the impactor a total mass (m_d) of 2.82 kg. The impactor was dropped at three different heights (H) as calculated by Eq. (1) to produce 5 J, 7.5 J and 10 J energy (E) upon impact to the specimens.

$$H = \frac{E}{m_d g}$$

alt-text: Fig. 2

Fig. 2



Experimental impact test set-up, a) Impact test fixture, b) impactor, c) specimen on the supporting block and held in place via 4 clamps, d) metallic insert to support the edges of laminates in the x direction and e) boundary conditions of the laminate under experiment.

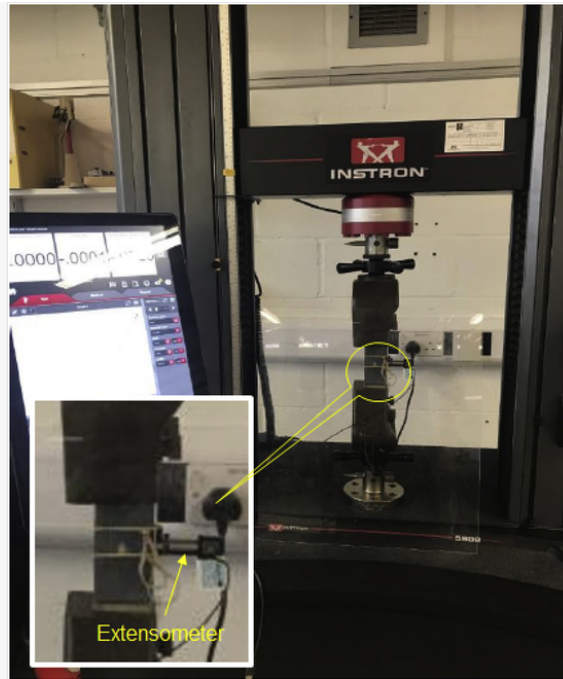
During test, a digital data acquisition unit was used to record the impact force-time curve history at 10 kHz frequency. It is worth noting that for any energy level, 12 tests were carried out, i.e. 3 for each configuration. Thus a total of 36 impact tests were carried out in this study.

3.3 Tensile test fixture

Quasi-static tensile tests were carried out on both the pristine and impacted specimens using an INSTRON tensile machine with a maximum load capacity of 100 kN, Fig. 3. A tensile loading rate of 2 mm/min was adopted based on recommendations specified in ASTM D3039. An extensometer was attached to the mid-gauge length of each specimen to record strain during each tensile experiment. It should be noted that for each energy level, 12 tests were carried out, i.e. 3 for each configuration. Thus, a total of 48 tensile tests were carried out, including pristine samples.

alt-text: Fig. 3

Fig. 3



Tensile test fixture.

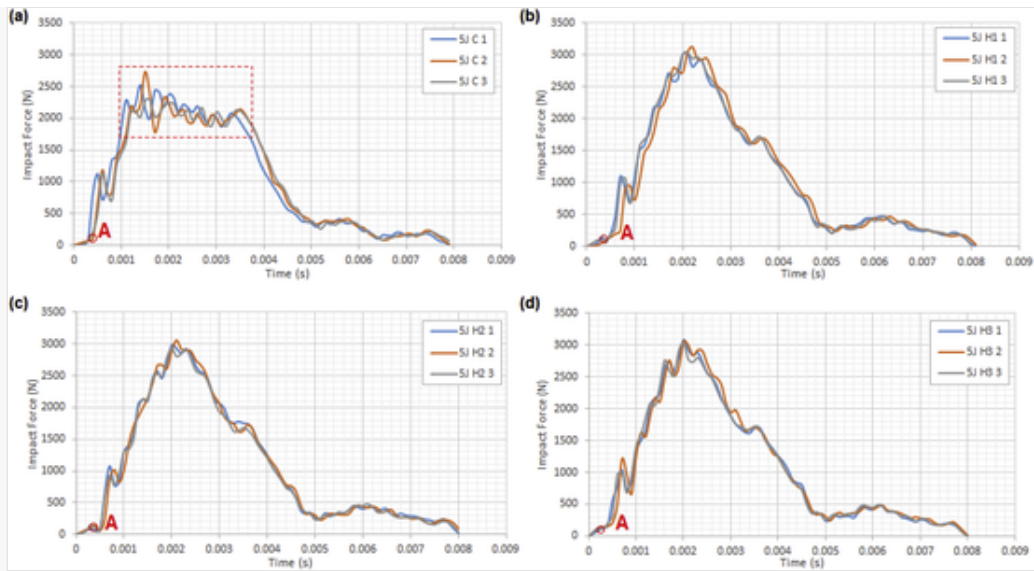
4 Results and discussions

4.1 Drop weight impact analysis and damage size

The impact force-time (F-T) curves and associated damage sizes for all energy levels are shown in Fig. 4 through to Fig. 10. The F-T curves provide damage initiation and growth regarding the low velocity impact behaviour of the different configurations. As illustrated in Figs. 4–6 and summarised in Table 3, consistent F-T history is observed for all energy levels. From the figures, the contact force in general decreases with increasing impact energy. All F-T curves except for 5J impact of H laminates demonstrated irregular behaviour or otherwise known as impact force perturbations after first impact. Such impact force perturbations that are associated with the delamination, fibre and matrix damage within plies, i.e. damage propagation [33], were observed by Zhou et al. [8] in which the boundary conditions were similar to this research. On the other hand, similar to Aktas et al. [34], the time at the peak contact force decreased with the increasing impact energy. For all energy levels, the initial segment of the graph is linear up to the point *A* (see Fig. 4a). At this point, which is regarded as the Hertzian failure point, damage begins mainly in the form of matrix cracking and inter-laminar delamination. For 5J impact, this point lies at 0.075kN for all laminates mainly as a result of similar resin content. Examining Fig. 4 and summarised results of Table 3, the 5J impact cases, the impact force peaks are at 2.518kN, 3.069kN, 2.994kN and 3.058kN for the C, H1, H2 and H3 configurations, respectively, with each F-T curve reducing to zero at approximately 0.008 s. This suggests full rebound of the impactor after impact.

alt-text: Fig. 4

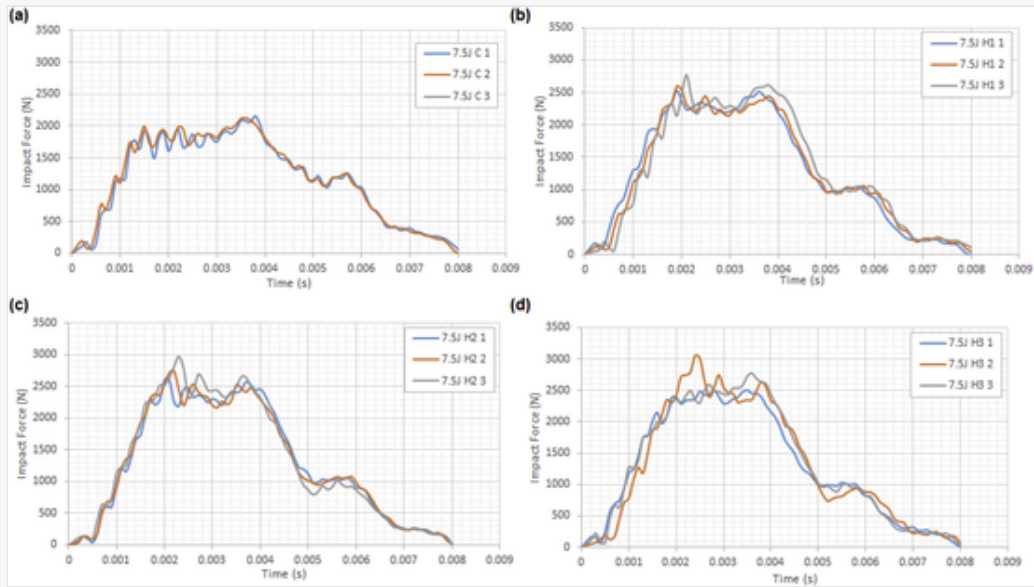
Fig. 4



Impact load curves under 5J energy level for (a) C, (b) H1, (c) H2 and (d) H3 samples.

alt-text: Fig. 5

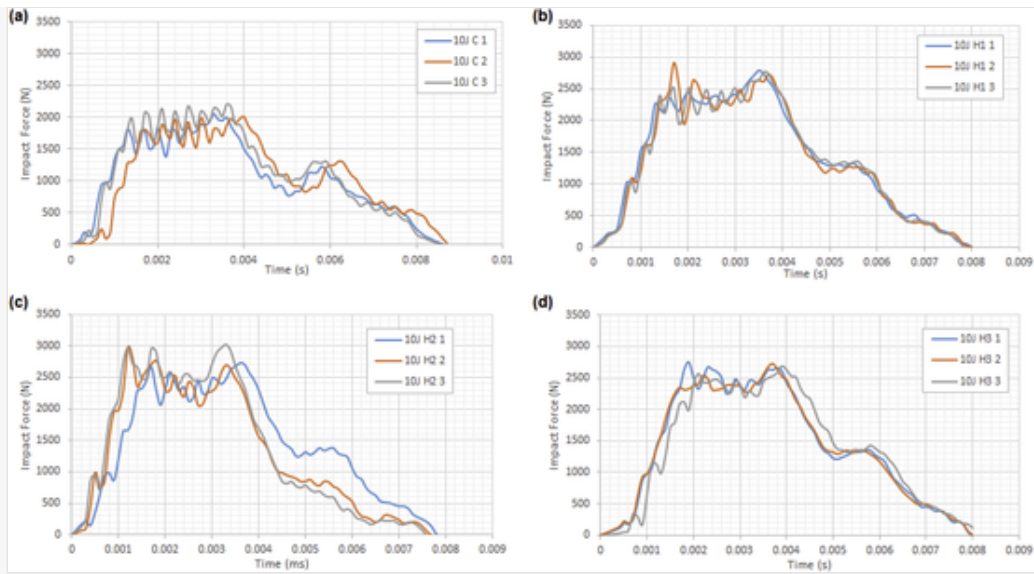
Fig. 5



Impact load curves under 7.5J energy level for (a) C, (b) H1, (c) H2 and (d) H3 samples.

alt-text: Fig. 6

Fig. 6



Impact load curves under 10J energy level for (a) C, (b) H1, (c) H2 and (d) H3 samples.

alt-text: Table 3

Table 3

i The presentation of Tables and the formatting of text in the online proof do not match the final output, though the data is the same. To preview the actual presentation, view the Proof.

Summary of impact F-T curves, damage sizes and spread angle.

Parameter	Impact Energy (Joules)	Units	C	H1	H2	H3
Average peak impact force	5	kN	2.518 ^a ±0.224	3.069 ± 0.053	2.994 ± 0.064	3.058 ± 0.026
Radius of damage on top surface		mm	5.70	12.00	17.60	11.00
Radius of damage on bottom surface		mm	15.00	16.80	17.40	17.00
Damage spread angle (α)		Deg	71.01	54.69	-3.36	60.46
Average peak impact force	7.5	kN	2.183 ± 0.072	2.633 ± 0.127	2.772 ± 0.184	2.778 ± 0.276
Radius of damage on top surface		mm	8.80	11.50	15.00	10.20
Radius of damage on bottom surface		mm	20.00	16.90	17.90	17.00
Damage spread angle (α)		Deg	74.05	57.80	40.46	63.43

Average peak impact force	10	kN	2.090 ± 0.101	2.624 ± 0.08	2.609 ± 0.159	2.725 ± 0.031
Radius of damage on top surface		mm	13.00	12.20	20.10	12.00
Radius of damage on bottom surface		mm	24.00	16.00	20.80	19.70
Damage spread angle (α)		Deg	73.77	48.18	11.63	66.17

Table Footnotes
^aThe number after ± represents standard deviation values.

Table 4 summarises the analytical membrane (k_m) and bending stiffness (k_b) of the pristine laminates. In the table, parameters β and η are dimensionless values determined by the boundary conditions of laminates based on thin circular plate theory. The reader is referred to Refs. [35,36] for detailed information of the formulation used. From Table 4, it is evident that the pristine C laminates have higher membrane and bending stiffness compared to the pristine H laminates. Despite being stiffer, the C laminates experienced lower force for all energy levels than the H laminates. For 5 J and 7.5 J impact, this led to smaller damage areas (see Figs. 7–10) on the impact side (top) of the C laminates compared to the H laminates. For 5 J impact, a distinctive irregular behaviour on the descending part of the F-T curve for C laminates (see red dashed rectangle in Fig. 4a) suggests that they were experiencing fibre breakage and large damage mainly in the form of delamination (see Fig. 8) away from the impact side such as through thickness delamination. As illustrated in Fig. 4b and c, the hybrid laminates did not exhibit this behaviour. It is noted that delaminations in the C laminates as shown in Fig. 8 were more visible at the interface closer to the centre of the plate thickness due to the maximum shear stress present resulting from their transverse bending. However, for higher impact energies (7.5 and 10 J) the irregular behaviour was observed for both C and H laminates and indicates that similar to C laminates, H laminates started to experience damage such as fibre breakage and delamination as evidenced in Figs. 9 to 10.

alt-text: Table 4

Table 4

 The presentation of Tables and the formatting of text in the online proof do not match the final output, though the data is the same. To preview the actual presentation, view the Proof.

Homogenised analytical membrane and bending stiffness of pristine laminates.

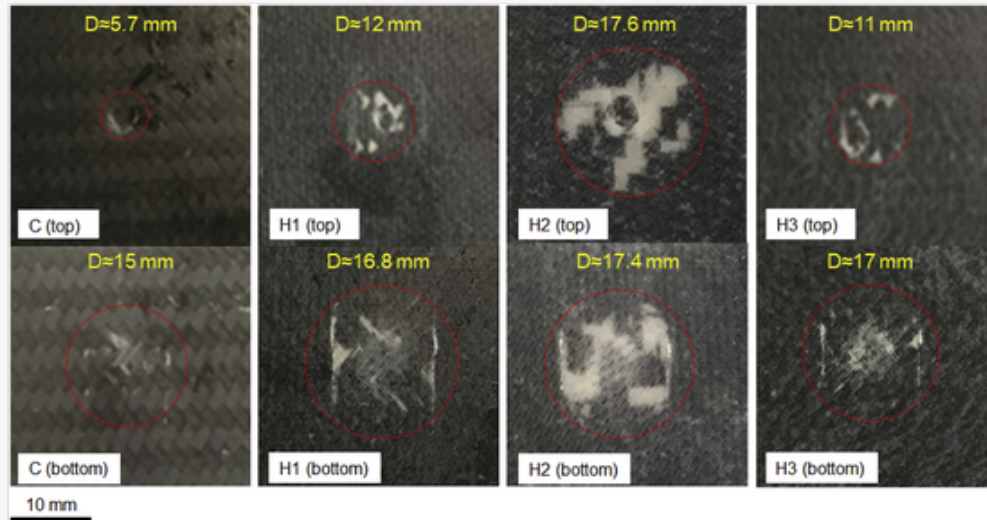
Parameter	Units	C	H1	H2	H3
t	mm	1.6	1.7	1.7	1.7
E_{xx}	GPa	56.5	39.7	47.6	39.7
D^*	N.mm	21144.98	15052.58	12597.58	16536.71

k_m^{**}	N/mm	222.94β	166.61β	199.63β	166.61β
K_b^{***}	N/mm	$405.98/\eta$	$289.01/\eta$	$241.87/\eta$	$317.50/\eta$

* $D \approx \sqrt{\frac{D_{11}D_{22}(1+\gamma)}{2}}$; $\gamma = \frac{D_{12}+2D_{66}}{\sqrt{D_{11}D_{22}}}$, ** $k_m \approx \beta \frac{\pi E_{xx} t}{4a^2}$, *** $k_b \approx \frac{E_{xx} t^3}{\eta a^2}$; $a = 50\text{mm}$ [35].

alt-text: Fig. 7

Fig. 7



Visual damage and size on top (impact side) and bottom of (a) C, (b) H1, (c) H2 and (d) H3 laminates for 5 J energy level.

alt-text: Fig. 8

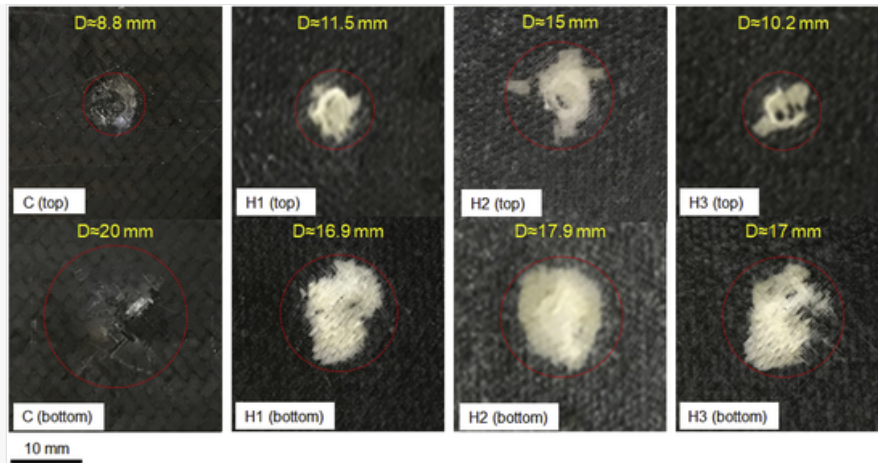
Fig. 8



Filtered side view of C laminate after 5 J impact showing multiple delaminations.

alt-text: Fig. 9

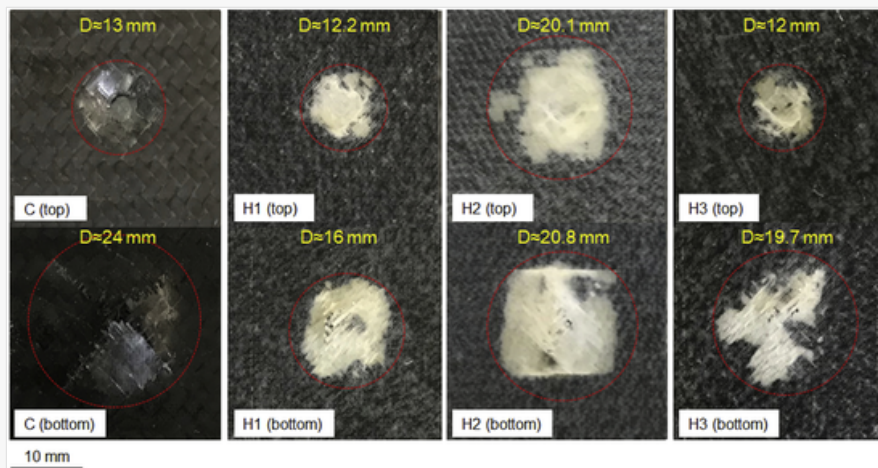
Fig. 9



Visual damage and size on top (impact side) and bottom of C, H1, H2 and H3 laminates for 7.5 J energy level.

alt-text: Fig. 10

Fig. 10

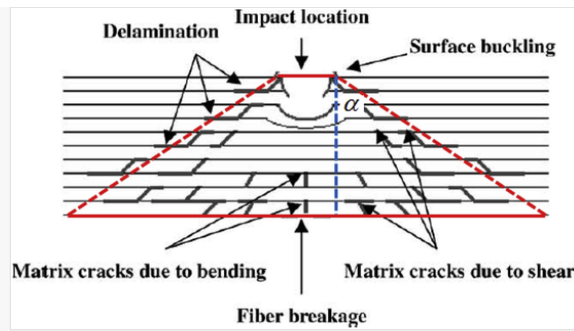


Visual damage and size on top (impact side) and bottom of C, H1, H2 and H3 laminates for 10 J energy level.

A typical laminate damage mode resulting from low velocity impact is schematically illustrated in Fig. 11. Based on the literature [37–39], the delaminations may be assumed to be circular in shape and their size may be approximated to increase linearly from the top to the bottom surface with a spread angle of α . For all energy levels, the approximate average spread angle across all energy levels was 73° , 54° , 16° and 63° for C, H1, H2 and H3 laminates, respectively. Spread angle for each energy level is summarised in Table 3. Hence, the H laminates showed a noted enhanced ability to contain their through thickness damage to the contact zone of the impact, compared to the C laminates.

alt-text: Fig. 11

Fig. 11



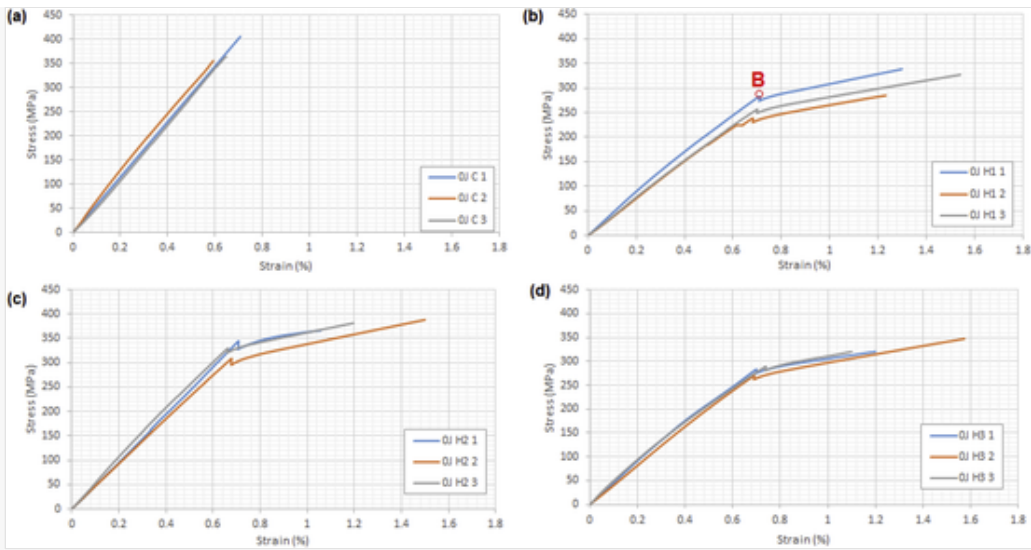
Schematic representation shows a typical impact damage mode for composite laminates [47].

4.2 Load displacement curves under tensile loading (TAI tests)

Tensile strength, failure strain and stiffness of both pristine and impacted laminates under various impact energy levels are shown in Fig. 12 to Fig. 15. The summary of these values is tabulated in Table 5 and graphically presented in Fig. 16. As shown in Fig. 12, the hybridisation of the pristine C laminates led to more pseudo-ductile behaviour with the average strain to failure of the H laminates increasing by approximately 200% compared to the C laminates. In other words, the stress-strain curve for the C laminates showed an abrupt failure whereas the thin hybrid laminates demonstrated an approximately bilinear response to loading. The first phase (up to point B as shown in Fig. 12b) is associated with loading of both carbon and glass plies without any failure. However, as the result of the higher load carrying capacity and small failure strain of the stiffer carbon plies, these plies failed at strains similar to that of C laminates, i.e. approximately 0.6% strain. Therefore, the stiffness of these laminates decreased which is characterised by a sudden load drop after point B where the load of the failed carbon plies was redistributed to the glass plies. Due to the high strain to failure of the glass plies, the final strain of the H laminates significantly extended beyond that of the C laminates. This favourable mechanism could be regarded as a valuable damage containment capability of the less brittle glass plies. These findings are in close agreement with those of refs. [40,41].

alt-text: Fig. 12

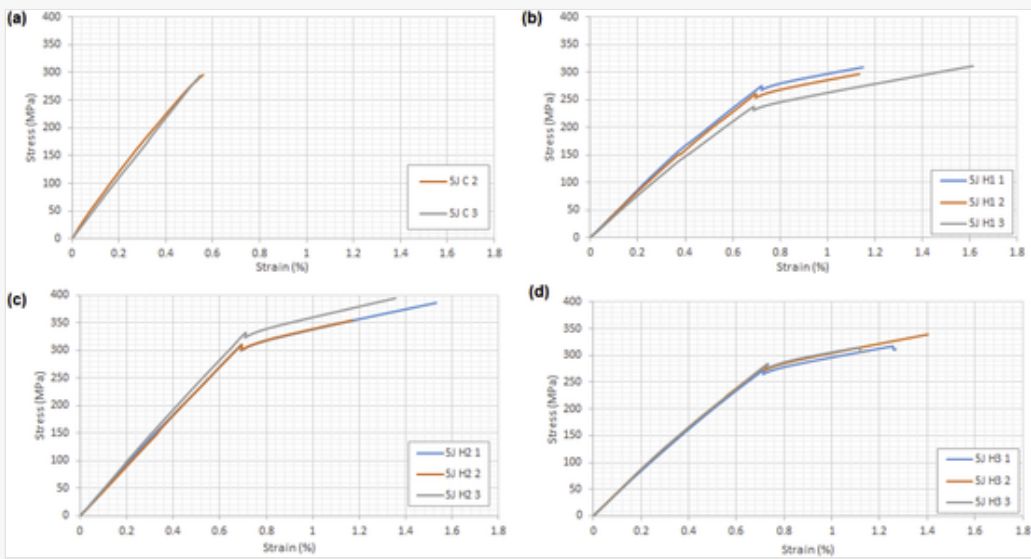
Fig. 12



Tensile stress-strain curves for pristine C, H1, H2 and H3 laminates.

alt-text: Fig. 13

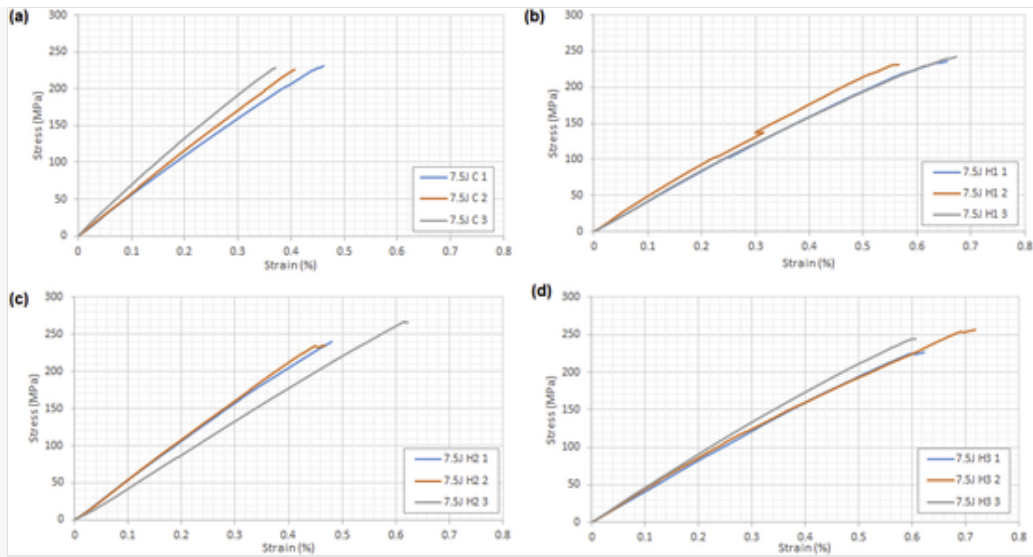
Fig. 13



Tensile stress-strain curves for C, H1, H2 and H3 laminates after 5J energy level.

alt-text: Fig. 14

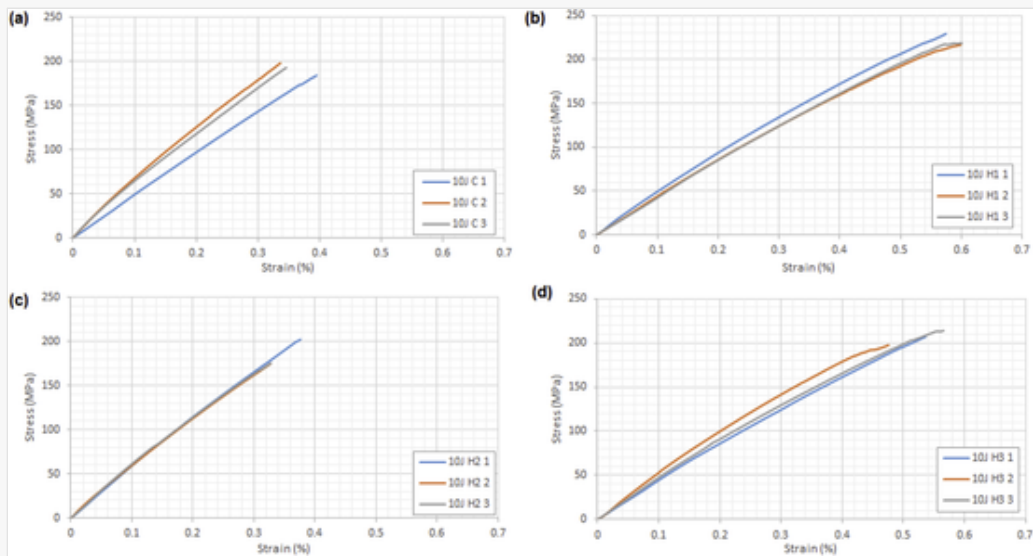
Fig. 14



Tensile stress-strain curves for C, H1, H2 and H3 laminates after 7.5 J energy level.

alt-text: Fig. 15

Fig. 15



Tensile stress-strain curves for C, H1, H2 and H3 laminates after 10 J energy level.

alt-text: Table 5

Table 5

i The presentation of Tables and the formatting of text in the online proof do not match the final output, though the data is the same. To preview the actual presentation, view the Proof.

Average homogenised Young's modulus, failure stress and strain of C, H1, H2 and H3 laminates.

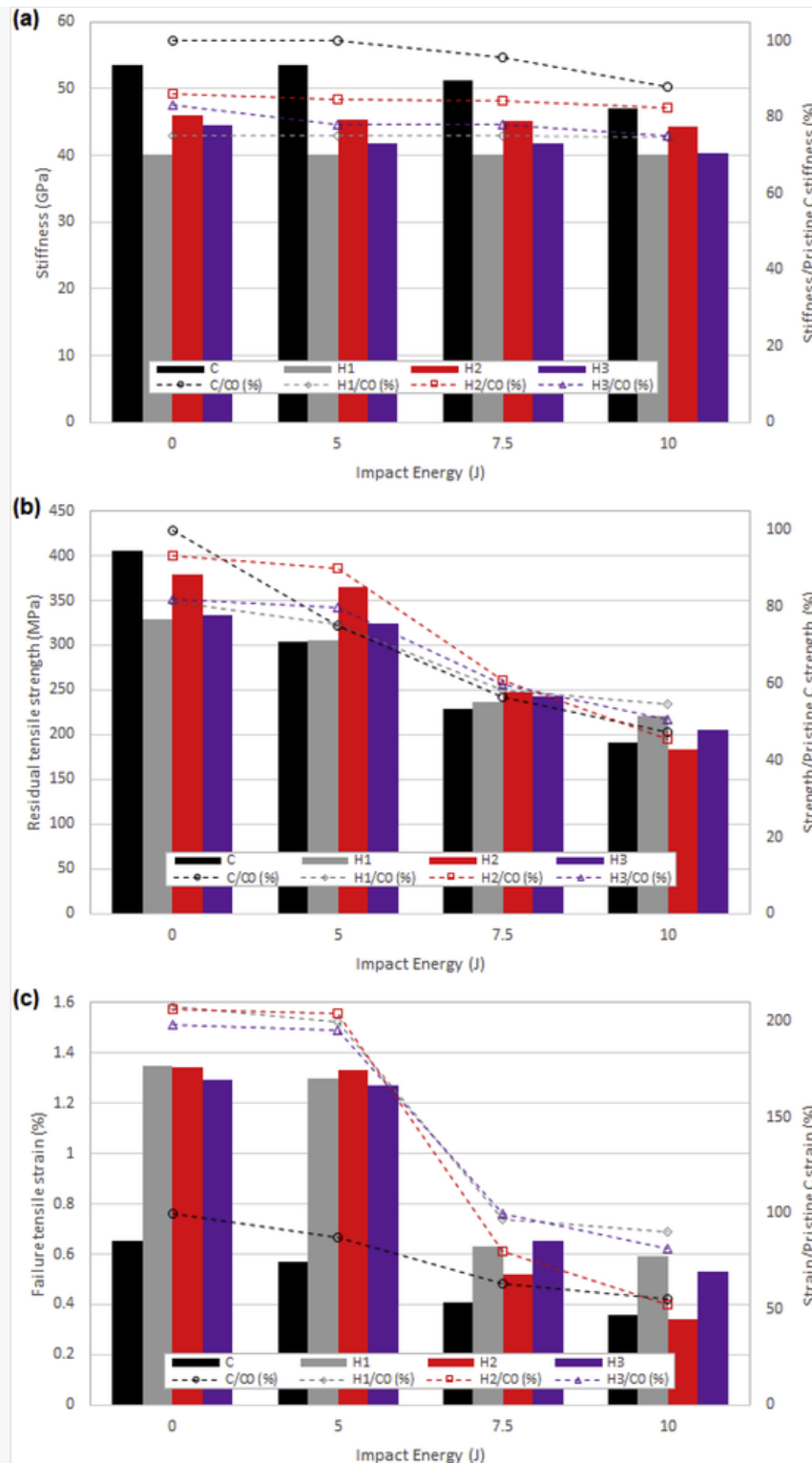
Parameter	Units	Impact Energy (Joules)	C	H1	H2	H3
Stiffness (E_{xx})	GPa	0	53.5 ± 6.57^a	40.2 ± 2.8	46.0 ± 1.33	44.5 ± 2.66
Failure stress	MPa		405.5 ± 26.85	329.3 ± 8.99	378.5 ± 11.33	333.0 ± 19.32
Failure strain	%		0.65 ± 0.06	1.35 ± 0.17	1.34 ± 0.22	1.29 ± 0.24
Stiffness (E_{xx})	GPa	5	53.5 ± 1.25	40.2 ± 2.95	45.3 ± 1.99	41.8 ± 0.83
Failure stress	MPa		304.0 ± 11.55	305.3 ± 7.93	365.3 ± 21.26	323.7 ± 13.51
Failure strain	%		0.57 ± 0.01	1.30 ± 0.27	1.33 ± 0.18	1.27 ± 0.13
Stiffness	GPa	7.5	51.2 ± 5.44	40.2 ± 2.51	45.1 ± 5.40	41.8 ± 1.95
Failure stress	MPa		228.6 ± 2.36	236.6 ± 5.45	247.5 ± 17.23	242.8 ± 15.09
Failure strain	%		0.41 ± 0.04	0.63 ± 0.06	0.52 ± 0.08	0.65 ± 0.06
Stiffness	GPa	10	47.1 ± 5.75	40.1 ± 2.07	44.2 ± 0.56	40.3 ± 4.42
Failure stress	MPa		191.5 ± 7.00	221.7 ± 6.78	184.0 ± 15.75	205.9 ± 8.27
Failure strain	%		0.36 ± 0.03	0.59 ± 0.01	0.34 ± 0.03	0.53 ± 0.04

Table Footnotes

^aThe number after \pm represents standard deviation values.

alt-text: Fig. 16

Fig. 16



The trend of change of a) stiffness, b) residual tensile strength and c) failure strain of C, H1, H2 and H3 laminates under various impact energy levels. Bar charts show the actual values (with primary vertical axis on left) and line charts demonstrate % of change with respect to pristine C values (with secondary vertical axis on right), i.e. C0.

Tensile testing of specimens after 5J impact energy level (Fig. 13) illustrated similar qualitative behaviour as that of pristine samples. However, as the impact energy level increased to 7.5J and 10J as shown in Figs. 14 and 15, respectively, the distinguishable bilinear response of the hybrid laminates diminished. In other words,

the increased impact energy reduced the hybrid laminates stiffness, and altered the failure behaviour, with their behaviour tending to the single stiffness and failure behaviour of the non-hybrid configurations. The reduction in the stiffness values can also be seen in [Table 1](#). This is due to the GFRP plies suffering significant damage under higher energy impacts and thus not being able to continue to bear much load beyond the strain at which the carbon plies fail. This behaviour is in line with the industrial practice of ignoring the load bearing capacity of GFRP plies located at the surface of commercial aircraft wing skins.

Based on [Fig. 16a](#), stiffness values of the C laminates were consistently higher than the H laminates for all energy levels. However, the C laminates exhibited more sensitivity to impact. Unlike the H laminates, as the impact energy level increased, the stiffness of the C laminates decreased consistently. [Fig. 16b](#) shows the change of residual tensile strength for pristine and impacted laminates. The trend suggests that despite the higher initial tensile strength of the pristine C laminates, their residual strength dropped significantly - by 75%, 56% and 47% for impact energies of 5 J, 7.5 J and 10 J, respectively. The residual tensile strength of the H1 and H3 laminates demonstrated less sensitivity to impact - with average strength reductions of 97%, 71% and 64% for impact energies of 5 J, 7.5 J and 10 J, respectively. Interestingly, the H2 laminates displayed similar strength percentage reduction as the C laminates but had 120% and 108% higher residual strength than the C laminates for energy levels of 7.5 J and 10 J, respectively. Additionally, for the highest energy level of this study, H1 and H3 laminates had 107% higher strength than the C and H2 laminates. This observation suggests that for higher energy levels, scattering glass laminates through the thickness is favourable to the residual tensile strength which is in agreement with findings of Zhou et al. [8]. [Fig. 16c](#) shows that the H laminates have considerably higher failure strains for the lowest energy impact (5 J). However, with higher energy impacts the failure strain reduces sharply for all of the H laminates - by averages of 45% and 36% for 7.5 J and 10 J impact, respectively. On the other hand, the C laminates despite having lower initial failure strain than the H laminates, do not display a sharp reduction in their failure strain with impacts greater than 5 J, [Fig. 16c](#). This could be associated with the fact that damage inflicted upon the GFRP plies in the form of matrix cracks and fibre failure, particularly those placed at the outer mould, decreased the ability of such plies to contribute their high strain to failure capability in the laminate fail. Hence, the significant reduction in overall failure strain of the H laminates was observed with impacts above 5 J.

4.3 Results summary and discussion

The following key characteristics can be drawn from the extensive experimental results:

- The hybrid laminates were able to contain the damage close to the impact surface whereas the spread of damage in the non-hybrid laminates was severe.
- The hybrid laminates experienced larger damage areas on the impact surface and a much smaller damage area on the bottom surface than the non-hybrid laminates.
- For the hybrid laminates, the through-thickness positioning of glass plies alters the damage size and spread distribution of damage through the thickness. Positioning the glass plies on the outer/inner mould surfaces (as a protective layer) resulted in much larger impact damage compared to the hybrid configurations with sub-surface glass plies. However, the surface glass plies reduced the spread of damage to the bottom surface whereas through-thickness

distribution of glass fibres led to smaller damage on the impacted surface with a much larger damage spread angle, most probably due to more evenly distribution of inter-laminar damage between the glass and carbon plies due to mismatch of their mechanical properties.

- The hybridisation of the laminates reduced both the stiffness and tensile strength compared to the pure carbon ply laminates, but resulted in a pseudo-ductile behaviour in stress-strain response and enhanced the failure to strain by almost 200%.
- Hybridisation led to a bilinear ductile tensile stress-strain curve for both pristine and low energy impacted (5 J) specimens. However, for higher energy impacted specimens (7.5 J and 10 J) this behaviour disappeared as a result of impact damage to the glass plies.
- Hybridisation led to little sensitivity in the laminate stiffness to the point that on average 95.4% of the pristine laminate stiffness was maintained after a 10 J impact. In the case of the purely carbon laminates, only 88% of the stiffness is retained after 10 J impact.
- As compared to pure C laminates, failure strain of the hybrid laminates was 200% higher for both the pristine and the 5 J impacted specimens but reduced sharply for higher energy levels (7.5 J and 10 J), with behaviour similar to that of the non-hybrid laminates.
- Scattering glass plies through the thickness as opposed to clustering them on the inner and outer mould surfaces was favourable for both the residual tensile strength and failure strains.
- The tensile strength of the non-hybrid laminates reduced by 25%, 43% and 52%, whereas the hybrid laminates reduced by 4%, 30% and 41% for 5 J, 7.5 J and 10 J energy impacts, respectively.

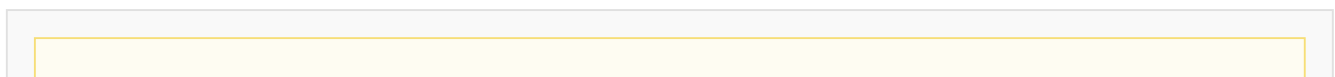
5 Conclusions

Although much work has considered hybridised Carbon and Glass Fibre Reinforced Polymers to positively influence the performance of composite structures when subjected to transvers impact loading, there is limited understanding considering low energy impact levels (≤ 10 J). Herein a detailed experimental study on the tensile performance of hybrid composite materials subjected to a graduated range of low energy level impacts has been presented. The experimental results establish how the hybrid layup influences the scale and form of damage. At the lowest impact energy examined (5 J) hybridisation led to a bilinear ductile tensile stress-strain curve and high strain to failure. However, at higher impact energies this behaviour ceases as a result of the impact damage to the glass plies. By distributing the glass plies through the laminate, as opposed to clustering the glass plies at the inner or outer mould surfaces, more favourable residual tensile strength and failure strains are possible.

Appendix A Supplementary data

Supplementary data to this article can be found online at <https://doi.org/10.1016/j.compositesb.2019.107537>.

References





- [1] Fierro GPM, Meo M. Nonlinear elastic imaging of barely visible impact damage in composite structures using a constructive nonlinear array sweep technique. *Ultrasonics* 2018;90:125–143.
- [2] Mikulik Z, Haase P. CODAMEIN-Composite Damage Metrics and Inspection (high energy blunt impact threat). *Eur. Aviat. Saf. Agency* 2012;1–106.
- [3] Park H, Kong C. Experimental study on barely visible impact damage and visible impact damage for repair of small aircraft composite structure. *Aero Sci Technol* 2013;29(1):363–372.
- [4] Imperiale VA, Cosentino E, Weaver PM, Bond IP. Compound joint: a novel design principle to improve strain allowables of FRP composite stringer run-outs. *Compos. Part A Appl Sci Manuf* 2010;41(4):521–531.
- [5] Mitrevski T, Marshall IH, Thomson R, Jones R, Whittingham B. The effect of impactor shape on the impact response of composite laminates. *Compos Struct* 2005;67(2):139–148.
- [6] Tirillò J, et al. High velocity impact behaviour of hybrid basalt-carbon/epoxy composites. *Compos Struct* 2017;168:305–312.
- [7] Mili F, Necib B. The effect of stacking sequence on the impact-induced damage in cross-ply E-glass/epoxy composite plates. *Arch Appl Mech* 2009;79(11):1019–1031.
- [8] Zhou J, Liao B, Shi Y, Zuo Y, Tuo H, Jia L. Low-velocity impact behavior and residual tensile strength of CFRP laminates. *Compos B Eng* 2019;161:300–313.
- [9] Czanocki P. Delamination resistance of laminates with various stacking sequences against low velocity impacts. *26th Symposium on Experimental Mechanics of Solids*, 240; 2016. p. 143–148.
- [10] Cestino E, Romeo G, Piana P, Danzi F. Numerical/experimental evaluation of buckling behaviour and residual tensile strength of composite aerospace structures after low velocity impact. *Aero Sci Technol* 2016;54:1–9.
- [11] Koricho EG, Khomenko A, Haq M, Drzal LT, Belingardi G, Martorana B. Effect of hybrid (micro- and nano-) fillers on impact response of GFRP composite. *Compos Struct* 2015;134:789–798.
- [12] da Silva Junior JEL, Paciornik S, d’Almeida JRM. Evaluation of the effect of the ballistic damaged area on the residual impact strength and tensile stiffness of glass-fabric composite materials. *Compos Struct* 2004;64(1):123–127.
- [13] Kazemahvazi S, Nilsson M, Zenkert D. Residual strength of GRP laminates with multiple randomly distributed fragment impacts. *Compos. Part A Appl Sci Manuf* 2014;60:66–74.

- [14] Wang Q, Yang Y, Jiang H, Liu CT, Ruan HH, Lu J. Superior tensile ductility in bulk metallic glass with gradient amorphous structure. *Sci Rep* Apr. 2014;4:4757.
- [15] Papa I, Ricciardi MR, Antonucci V, Lopresto V, Langella A. Impact performance of GFRP laminates with modified epoxy resin. *Procedia Eng* 2016;167:160–167.
- [16] Naik NK, Ramasimha R, Arya H, Prabhu SV, ShamaRao N. Impact response and damage tolerance characteristics of glass-carbon/epoxy hybrid composite plates. *Compos. Part B Engineering* 2001;32(7):565–574.
- [17] V Hosur M, Abdullah M, Jeelani S. Studies on the low-velocity impact response of woven hybrid composites. *Compos Struct* 2005;67(3):253–262.
- [18] Sevkat E, Liaw B, Delale F, Raju BB. Drop-weight impact of plain-woven hybrid glass–graphite/toughened epoxy composites. *Compos. Part A Appl Sci Manuf* 2009;40(8):1090–1110.
- [19] Liu H, Falzon BG, Tan W. Predicting the Compression-After-Impact (CAI) strength of damage-tolerant hybrid unidirectional/woven carbon-fibre reinforced composite laminates. *Compos. Part A Appl Sci Manuf* 2018;105:189–202.
- [20] He W, Liu J, Wang S, Xie D. Low-velocity impact response and post-impact flexural behaviour of composite sandwich structures with corrugated cores. *Compos Struct* 2018;189:37–53.
- [21] Yahaya R, Sapuan SM, Jawaid M, Leman Z, Zainudin ES. Measurement of ballistic impact properties of woven kenaf–aramid hybrid composites. *Measurement* 2016;77:335–343.
- [22] Jalalvand M, Czél G, Wisnom MR. Numerical modelling of the damage modes in UD thin carbon/glass hybrid laminates. *Compos Sci Technol* 2014;94:39–47.
- [23] Fotouhi M, Jalalvand M, Wisnom MR. High performance quasi-isotropic thin-ply carbon/glass hybrid composites with pseudo-ductile behaviour in all fibre orientations. *Compos Sci Technol* Nov. 2017;152:101–110.
- [24] Czél G, et al. Pseudo-ductility and reduced notch sensitivity in multi-directional all-carbon/epoxy thin-ply hybrid composites. *Compos. Part A Appl Sci Manuf* Jan. 2018;104:151–164.
- [25] Czél G, Wisnom MR. Demonstration of pseudo-ductility in high performance glass/epoxy composites by hybridisation with thin-ply carbon prepreg. *Compos. Part A Appl Sci Manuf* 2013;52:23–30.
- [26] Wisnom MR. The role of delamination in failure of fibre-reinforced composites. *Philos Trans R Soc A Math Phys Eng Sci* 2012.
- [27] Habibi M, Laperrière L, Hassanabadi HM. Influence of low-velocity impact on residual tensile properties of nonwoven flax/epoxy composite. *Compos Struct* Feb. 2018;186:175–182.

- [28] Reddy PRS, Reddy TS, Mogulanna K, Srikanth I, Madhu V, Rao KV. Ballistic impact studies on carbon and E-glass fibre based hybrid composite laminates. *Procedia Eng.* 2017;173:293–298.
- [29] Zhang J, Chaisombat K, He S, Wang CH. Hybrid composite laminates reinforced with glass/carbon woven fabrics for lightweight load bearing structures. *Mater Des* 2012;36:75–80.
- [30] Rhead AT, Hua S, Butler R. Damage resistance and damage tolerance of hybrid carbon-glass laminates. *Compos. Part A Appl Sci Manuf* 2015;76:224–232.
- [31] Santulli C. Mechanical and impact damage analysis on carbon/natural fibers hybrid composites: a review. *Materials* 2019;12(3).
- [32] Priyanka P, Dixit A, Mali HS. High-strength hybrid textile composites with carbon, kevlar, and E-glass fibers for impact-resistant structures. A review. *Mech Compos Mater Nov.* 2017;53(5):685–704.
- [33] Xu Z, Yang F, Guan ZW, Cantwell WJ. An experimental and numerical study on scaling effects in the low velocity impact response of CFRP laminates. *Compos Struct* 2016;154:69–78.
- [34] Aktas M, Karakuzu R, Icten BM. Impact behavior of glass/epoxy laminated composite plates at high temperatures. *J Compos Mater May* 2010;44(19):2289–2299.
- [35] Abisset E, Daghia F, Sun XC, Wisnom MR, Hallett SR. “Interaction of inter- and intralaminar damage in scaled quasi-static indentation tests: Part 1 – Experiments. *Compos Struct* Feb. 2016;136:712–726.
- [36] Singh H, Mahajan P. Analytical modeling of low velocity large mass impact on composite plate including damage evolution. *Compos Struct* 2016;149:79–92.
- [37] Olsson R. Analytical prediction of large mass impact damage in composite laminates. *Composites Part A Appl Sci Manuf* 2001;32(9):1207–1215.
- [38] Shyr TW, Pan YH. Impact resistance and damage characteristics of composite laminates. *Compos Struct* 2003.
- [39] Grammatikos SA, Kordatos EZ, Matikas TE, David C, Paipetis AS. Current injection phase thermography for low-velocity impact damage identification in composite laminates. *Mater Des* 2014.
- [40] Czél G, Jalalvand M, Wisnom MR. “Design and characterisation of advanced pseudo-ductile unidirectional thin-ply carbon/epoxy–glass/epoxy hybrid composites. *Compos Struct* 2016;143:362–370.
- [41] Wisnom MR, Czél G, Swolfs Y, Jalalvand M, Gorbatiikh L, Verpoest I. Hybrid effects in thin ply carbon/glass unidirectional laminates: accurate experimental determination and prediction. *Compos. Part A Appl Sci Manuf* 2016;88:131–139.

- [42] Meng Q, Wang Z. Modeling analysis of fiber hybridization in hybrid glass/carbon composites under high-velocity impact. *Polym Compos* 2015;38(11):2536–2543.
- [43] Ismail KI, Sultan MTH, Shah AUM, Jawaid M, Safri SNA. Low velocity impact and compression after impact properties of hybrid bio-composites modified with multi-walled carbon nanotubes. *Compos B Eng* 2019;163:455–463.
- [44] Dhakal HN, Ismail SO, Jiang C, Zhang Z, Sweatman T. Influence of barely visible impact damage on post-impact residual flexural properties of hybrid Fibri Rock – aero Eco-composites. *Mater Lett* 2018.
- [45] Andrew J, Ramesh C. Residual strength and damage characterization of unidirectional glass–basalt hybrid/epoxy CAI laminates. *Arabian J Sci Eng* 2015;40(6):1695–1705.
- [46] Farhood N, Karuppanan S, Ya H, Ovinis M. Effects of carbon fiber hybridization on the compressive strength of glass-carbon/epoxy hybrid composite pipes before and after low velocity impact. *Key Eng Mater* 2019;796:30–37.
- [47] Shyr T-WW, Pan Y-HH. Impact resistance and damage characteristics of composite laminates. *Compos Struct Nov.* 2003;62(2):193–203.

Appendix A Supplementary data

The following is the Supplementary data to this article:

[Multimedia Component 1](#)

Multimedia component 1

Queries and Answers

Query: Your article is registered as a regular item and is being processed for inclusion in a regular issue of the journal. If this is NOT correct and your article belongs to a Special Issue/Collection please contact n.thandavamoorthy@elsevier.com immediately prior to returning your corrections.

Answer: Yes

Query: Please confirm that given names and surnames have been identified correctly and are presented in the desired order and please carefully verify the spelling of all authors' names.

Answer: Yes

Query: Please confirm that the provided email “mahdi.damghani@uwe.ac.uk” is the correct address for official communication, else provide an alternate e-mail address to replace the existing one, because private e-mail addresses should not be used in articles as the address for communication.

Answer: I can confirm that "mahdi.damghani@uwe.ac.uk" is the correct email address.

Query: Correctly acknowledging the primary funders and grant IDs of your research is important to ensure compliance with funder policies. We could not find any acknowledgement of funding sources in your text. Is this correct?

Answer: This work was funded by University of the West of England under Vice-Chancellor's Early Career Researcher Awards (UEDM0150).

Query: Please provide the volume number or issue number or page range or article number for the bibliography in Ref(s). [26], [38], [39], [44].

Answer: [26] Wisnom MR. The role of delamination in failure of fibre-reinforced composites. *Philos Trans R Soc A Math Phys Eng Sci* 2012;370:1850–70. doi:10.1098/rsta.2011.0441.

[38] Shyr T-WW, Pan Y-HH. Impact resistance and damage characteristics of composite laminates. *Compos Struct* 2003;62:193–203. doi:10.1016/S0263-8223(03)00114-4.

[39] Grammatikos SA, Kordatos EZ, Matikas TE, David C, Paipetis AS. Current injection phase thermography for low-velocity impact damage identification in composite laminates. *Mater Des* 2014;55:429–41. doi:10.1016/j.matdes.2013.09.019.

[44] Dhakal HN, Ismail SO, Jiang C, Zhang Z, Sweatman T. Influence of barely visible impact damage on post-impact residual flexural properties of hybrid Fibri Rock – Aero Eco-composites. *Mater Lett* 2018;233:233–7. doi:10.1016/j.matlet.2018.09.036.